Scientific
Research

A Comparison of Control Methods for Z-Source Inverter

Cong-Thanh Pham[1,2], Anwen Shen[1], Phan Quoc Dzung[3], Nguyen Bao Anh[3], Nguyen Xuan Phu[3]

[1]Department of Control Science and Engineering, Huazhong University of Science and Technology, Wuhan, China
[2]Electrical & Electronics Engineering Faculty, HCMC University of Transport, Ho Chi Minh City, Vietnam
[3]HCMC University of Technology, Ho Chi Minh City, Vietnam
Email: phamcongthanh09@yahoo.com

ABSTRACT

In recent years, Z-source inverters (ZSI) have been proposed as a replacement power conversion concept which it has both voltage buck and boost abilities. In addition, ZSI doesn't require dead-time to protection short circuit at two switches any of the same phase leg in the inverter bridge and to achieve optimal harmonic of current, voltage. This paper presents two different control methods (CM) for ZSI. The aim of this study to compare between two modulation methods, there are modified space vector pulse width modulation method (MSVM) and the simple boost control (SBC) about the unique harmonic performance features, the total average and peak switching device power of the inverter system. In addition, this paper also analyzes about the ability exceed modulation index in linear region of two CM using MATLAB/Simulink.

Keywords: Buck-Boost; Current Source Inverters (CSIs); Pulse-Width Modulation (PWM); Voltage Source Inverters (VSIs); Z-Source Inverters (ZSI)

1. Introduction

In a conventional voltage source inverter, the two switches of any phase leg cannot be gated at the same time because this may cause a short circuit situation and thus destroy the inverter. In addition, the maximum output voltage cannot exceed the dc bus voltage. These limitations in such conventional voltage source inverter can be overcome by using ZSI [1], **Figure 1**.

A comparison among conventional pulse-width modulation (PWM) inverter, dc-dc boosted PWM inverter and ZSI but ZSI shows that higher efficiency and lower cost. Because of these reasons, ZSI has applied in hybrid electric vehicles [2,3]. In addition, in [4] show comparison among the traditional I-source inverter and (VSI) with the Z-source network should require less capacitance, inductance and size smaller than traditional dc-dc boosted PWM inverter. Therefore, these results in increasing attention on ZSI, especially for the application where the dc input source has a wide voltage variation range such as fuel cell, battery, lead acid. Also, the ZSI has applied for direct-drive wind generation system and photovoltaic power system base on tracking algorithm maximum power and hybrid electric vehicles [5-7].

Additionally, the maximum boost control is alike the conventional carrier-based PWM method base on all zero voltage vectors, shoot through state (the other zero vectors) and the six active states which are maintained unchanged but the main drawbacks of this modulation method is big inductor ripple and a large inductor when the output frequency is low. Therefor, they will increase the cost and size of the circuit [8].

Given its many benefits, many studies have been researched into CM of ZSI. Cosequently, how chose CM which highest efficiency is very important in control systems of ZSI. Through detailed analysis, the aim of this study to show how various two CM for ZSI, there are MSVM and the SBC which they are analyzed and compared about the unique harmonic features of current, voltage and the total average switching device power, the total peak switching device power of the inverter system. In addition, this paper also analyzes about the ability exceed modulation index in linear region of two CM using simulation MATLAB/Simulink.

2. Equivalent Circuit, Operating Principle and Total Switching Device Power of ZSI

2.1. Equivalent Circuit, Operating Principle of ZSI

In **Figure 1** show ZSI voltage-type configuration, which include inductors (L_1 and L_2) are similar inductance L,
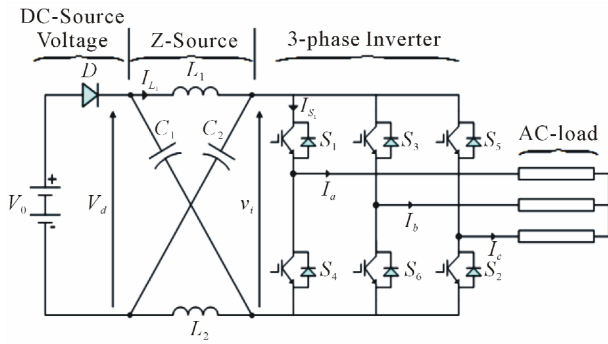
Figure 1. ZSI voltage-type configuration.

Figure 2. Equivalent circuits of ZSI. (a) Non-shoot-through mode; (b) Shoot-through mode.

simultaneously capacitors (C_1 and C_2) are similar capacitance C. Where L and C are connected in X shape, the dc input voltage source which may be fuel cell, battery or diode rectifier. The general inverter have two zero voltage vector and six active voltage vectors but in the three-phase ZSI has one additional zero voltage vector that is third zero state vector or the shoot-through zero state. The influence of this phase-leg shoot-through on the inverter performance can be considered the equivalent circuits shown in **Figure 2**. In operating principle of ZSI there are two operating modes: non-shoot-through mode and shoot-through mode. In non-shoot-through mode **Figure 2(a)** that the ZSI operates under the conventional PWM. The shoot-through state is forbidden in the conventional inverter but in the ZSI the shoot-through mode are given in **Figure 2(b)**. In **Figure 2(b)** show that the load terminals of any phase legs are shorted both the upper and lower. At that time, the dc capacitor voltage can be boosted to the desired value.

Where β is the angle between the reference voltage vector V_{ref} and voltage vector V_1. Because assume inductors (L_1 and L_2), capacitors (C_1 and C_2) have alike inductance (L) and capacitance (C) respectively, we have

$$\begin{cases} V_{C1} = V_{C2} = V_C \\ v_{L1} = v_{L2} = v_L \end{cases} \quad (1)$$

- Non shoot-through time internal of one period non shoot-through zero state for a period T_n in **Figure 2(a)**, we have:

$$\begin{cases} V_d = V_0 \\ v_L = V - V_C \\ v_i = V_C - v_L = 2V_C - V_0 \end{cases} \quad (2)$$

- Shoot-through time internal of one period shoot-through zero state for a period T_{sr} in **Figure 2(b)**, we have:

$$\begin{cases} v_i = 0 \\ v_L = V_C \\ V_d = 2V_C \end{cases} \quad (3)$$

where V_o is the dc source voltage and one period switching cycle T_{sf}, where $T_{sf} = T_{sr} + T_n$ and $M_{sr} = \dfrac{T_{sr}}{T_{sf}}$ is the shoot-through time duty ratio.

The average voltage of the inductors over one switching period should be zero in steady state, from (2) and (3) thus capacitor voltage can expressed:

$$V_{C1} = V_{C2} = V_C = \frac{1 - \dfrac{T_{sr}}{T_{sf}}}{1 - 2 \cdot \dfrac{T_{sr}}{T_{sf}}} \cdot V_d = \frac{1 - M_{sr}}{1 - 2 \cdot M_{sr}} \cdot V_d \quad (4)$$

$$V_i = \bar{v}_i = \frac{T_{sr} \cdot 0 + T_n (2 \cdot V_c - V_d)}{T_{sf}} = \frac{1 - M_{sr}}{1 - 2 \cdot M_{sr}} \cdot V_d = V_c \quad (5)$$

$$\hat{v}_i = V_c - V_L = 2 \cdot V_c - V_d = \frac{1}{1 - 2 \cdot M_{sr}} \cdot V_d \quad (6)$$

$$0 < M_{sr} < \frac{1}{2} \Rightarrow 0 < T_{sr} < \frac{T_{sf}}{2} \quad (7)$$

From (6), if M_{sr} is increase then $\hat{v}_i$ is also increase, where $\hat{v}_i$ is the voltage stress across switching devices.

2.2. Total Switching Device Power (*TSDP*)

In an inverter system, choice switching device must depend on the peak, average current and the maximum voltage impressed going through it. The switching device

power is introduced to quantify the voltage and current stress of an inverter system [8]. *TSDP* is a measure of the total semiconductor device requirement.

The total average switching device power of the inverter system $(TSDP)_{av}$ is given in [8]:

$$(TSDP)_{av} = 4\hat{v}_i \frac{P_o}{V_{op}} M_{sr} + \frac{2\sqrt{2} \cdot P_o \cdot \hat{v}_i}{\pi \hat{v}_{ac} \cos\varphi}(1 - M_{sr}) \quad (8)$$

The total peak switching device power of the inverter system $(TSDP)_{pk}$ is also given in [8]:

$$(TSDP)_{pk} = 4\hat{v}_i \frac{P_o}{V_{op}} + \frac{\sqrt{2} \cdot P_o \cdot \hat{v}_i}{\hat{v}_{ac} \cos\varphi} \quad (9)$$

where N is the number of switching devices used, I_L the inductor current, $\hat{v}_{ac}$ the output peak phase voltage from the inverter and P_o maximum power output of the DC-source voltage.

3. Proposed CM of MSVM and SBC

3.1. Proposed CM of MSVM

Nowadays, the space vector PWM (SVM) method have widely used at regulated PWM inverter due to a higher modulation index and lower current harmonics in [9]. The SVM is suitable to control the shoot-through time in ZSI. Where V_0, V_7 and shoot-through are zero vectors (in ZSI), where V_1 to V_6 are the six active vectors. If the reference voltage vector V_{ref} (the sinusoidal three-phase command voltage of output ZSI with minimum amount of harmonic distortion) is located between the arbitrary vector V_a and V_b, the reference voltage vector is divided into the two adjacent voltage vectors (V_a, V_b) and zero vectors $(V_0, V_7$ and shoot-through) in **Figure 3**. When V_{ref} rotate around section (1 - 6) of hexagon while (a, b) are changed: $(a, b) = (1, 2); (2, 3); (3, 4); (4, 5); (5, 6)$ in every sector, respectively. In one sampling interval, V_a and V_b are applied at times T_a and T_b, respectively, and the zero vector is applied at time $T_{sf} = (T_a + T_b) + T_0' + T_{sr}$ where $T_0' + T_{sr} = T_0$.

Consequently, from (10), the reference voltage vector V_{ref} can be given by

$$\overline{V}_{ref} = \overline{V}_a \cdot T_a + \overline{V}_b \cdot T_b \quad (10)$$

$$T_a = \sqrt{3} \frac{V_{ref}}{\hat{v}_i} \cdot T_{sf} \cdot \sin\left(\frac{\pi}{3} - \beta\right) \quad (11)$$

$$T_b = \sqrt{3} \frac{V_{ref}}{\hat{v}_i} \cdot T_{sf} \cdot \sin\beta \quad (12)$$

The conventional SVM in **Figure 4(a)** and the MSVM in **Figure 4(b)** where T_{sr} is shoot-through time has an extra for boosting the dc link voltage of the inverter beside time intervals T_a, T_b and T_0.
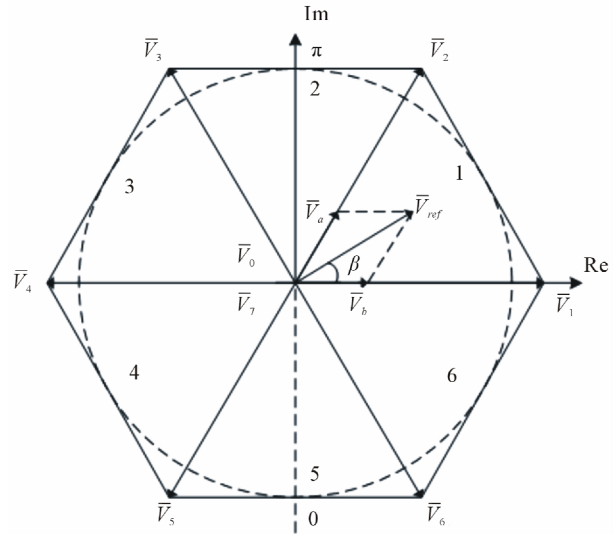
Figure 3. Voltage vector through conventional SVM of VSI.

From **Figure 4** the shoot-through states (STS) are evenly assigned to each phase with $\frac{2T}{3}$ within zero voltage period $\frac{T_0}{4}$ and $\frac{T}{3}$ within active voltage period $\frac{T_a}{2}$ and $\frac{T}{3}$ within active voltage period $\frac{T_b}{2}$, where T_a and T_b are unchanged. So the STS does not affect the SVM CM of the inverter, and it is limited to the zero state time T_0. Where T are determined by (13). Therefore, the STS should be inserted period intervals are maintained at the start and end of the switching cycle to achieve alike optimal harmonic performance.

$$T_{sr} = 6.2 \cdot \frac{T}{3} = 4 \cdot T \Rightarrow T = \frac{T_{sr}}{4} \quad (13)$$

From (7) we have

$$0 < T < \frac{T_{sf}}{8} \quad (14)$$

In the undermodulation region $(0 \le M \le M_{max})$.

Figure 3, V_{ref} always remains within hexagon in [10]. Let us define a modified modulation factor M given by

$$M = \frac{\hat{V}_{ref}}{\hat{V}_{1sw}} = \frac{\hat{V}_{ref}}{\frac{2}{\pi} \cdot \hat{v}_i} \quad (15)$$

where $\hat{V}_{ref}$ = vector magnitude (or phase peak value), in the linear region $\hat{V}_{ref}$ is the output peak phase voltage from the inverter $\hat{v}_{ac} (\hat{V}_{ref} = \hat{v}_{ac})$ and $\hat{V}_{1sw}$ = fundamental peak value $\left(\frac{2}{\pi} \cdot \hat{v}_i\right)$ of the square-phase voltage
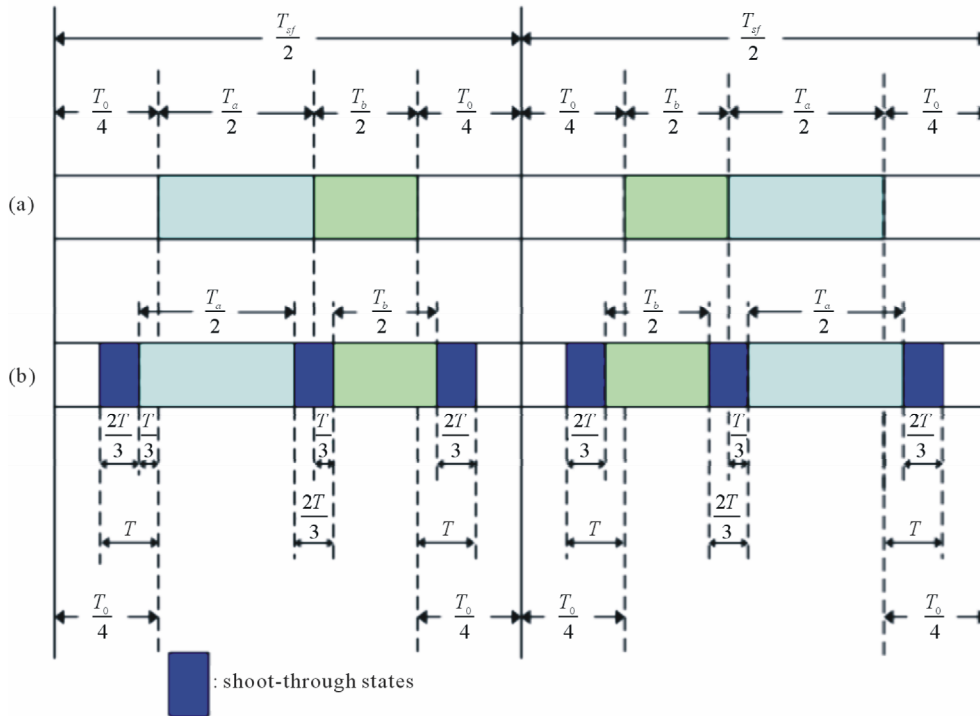
Figure 4. MSVM (a) Switching patterns for traditional SVM; (b) Switching patterns for MSVM.

wave. The maximum possible value of modulation factor $\left(M_{\max}\right)$ at the end of the under modulation region can derived. The radius $\left(\hat{V}_{refm}\right)$ **Figure 3** of the inscribed circle can be given as

$$M_{\max} = \frac{\hat{V}_{refm}}{\hat{V}_{1sw}} = \frac{\frac{2}{3} \cdot \hat{v}_i \cos\frac{\pi}{6}}{\frac{2}{\pi} \cdot \hat{v}_i} = \frac{\frac{1}{\sqrt{3}} \cdot \hat{v}_i}{\frac{2}{\pi} \cdot \hat{v}_i} \qquad (16)$$

This means that 90.7 percent of the fundamental at the square wave is available in the linear region.

3.2. The Simple Boost Control (SBC)

The SBC method strategy inserts STS in all the PWM conventional zero states during one switching period. The six active states are maintained unchanged as in the conventional carrier based PWM [2]. When the triangular waveform is greater than the upper envelope, V_{po}, or lower than the bottom envelope, V_{ne}, the circuit turns into shoot-through state, show **Figure 5**. The output peak phase voltage from the inverter can be given by

$$\hat{v}_{ac} = M_a \cdot \frac{\hat{v}_i}{2} = M_a \frac{1}{1 - 2 \cdot M_{sr}} \cdot \frac{V_d}{2} \qquad (17)$$

where M_a is the modulation index of magnitude $\left(0 \le M_a = \frac{\text{magnitude} - \text{sine}}{\text{magnitude} - \text{carrier}} \le 1\right)$ in [10]. At $M_a = 1$, M = modulation factor, in the linear region $(0 \le M \le M_{\max})$
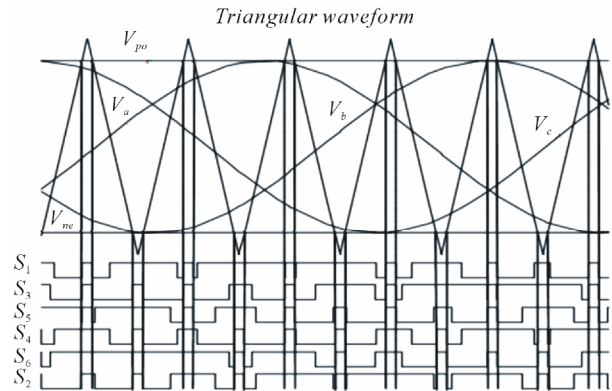
Figure 5. Simple boost control.

where $M_{\max}$ = maximum modulation factor determined by

$$M_{\max} = \frac{\hat{v}_{ac}}{\hat{V}_{1sw}} = \frac{\frac{1}{2} \cdot \hat{v}_i}{\frac{2}{\pi} \cdot \hat{v}_i} = 0.7855 \qquad (18)$$

At $M_a = 1$, the maximum value of fundamental peak voltage is $\frac{1}{2} \cdot \hat{v}_i$, Which is 78.55 percent of peak voltage $\left(\frac{2}{\pi} \cdot \hat{v}_i\right)$ of the square wave. From (16), (18) we can see that the maximum value of fundamental peak voltage of the MSVM method is higher than the SBC method.

Therefore, the MSVM method modulation index in linear can exceed more than the SBC method.

4. Simulation

To verify the validity of the above analysis, simulation models shown in **Figure 1** use Matlab/Simulink for MSVM and SBC methods of z-source inverter are analyzed. The simulation for two CMs with parameters are the same, see **Table 1**.

In **Figure 6** shows the inverter's dc link voltage, the ZSI's capacitor voltage and comparison with maximum output voltage of DC-source. We observe from the figure that the inverter's dc link voltage $(\hat{v}_i)$ boosted to (500 V) greater than maximum output of DC-source (400 V) is (100 V) see **Table 2**.

In **Figure 7** shows the switching output line voltage and phases voltage waveform of ZSI with MSVM methods. **Figures 8** and **9** show output line voltage and current sine waveforms of ZSI with MSVM and SBC methods, respectively.

Output line peak voltage and peak current sine waveforms of ZSI with MSVM method greater than output line peak voltage and peak current sine waveforms of ZSI with SBC method, respectively.

Figures 10 and **11** show total harmonic disturbance spectra of output line voltage $(THD)_U$ and total harmonic disturbance spectra of output current $(THD)_I$ which $(THD)_I$ and $(THD)_U$ of MSVM method less than $(THD)_I$ and $(THD)_U$ of SBC method. These results are given in **Table 2**. Also in **Table 2** show calculate results of MSVM and SBC methods use Equations (4)-(18). $(TSDP)_{av}$, $(TSDP)_{pk}$ of MSVM method less than $(TSDP)_{av}$, $(TSDP)_{pk}$ of SBC method.

In the future, we will apply MSVM for ZSI in many control systems (e.g. motor speed control system, hybrid electric vehicles, photovoltaic, direct-drive wind generation system). In **Figure 12** shows the figure experiments for motor speed control system.

5. Acknowledgements

Table 1. Parameters are used for simulation of MSVM and SBC.

Parameter	Value
Z-source inductance (L_1 and L_2)	1.5 mH
Z-source capacitance (C_1 and C_2)	1000 μF
Load resistance	10 Ω
Load inductance	0.025 mH
Switching frequency (f_{sf})	10 kHz
Fundamental frequency (f_1)	60 Hz
Maximum power output of the DC-source voltage (P_0)	3700 W
Output DC-source voltage at maximun power (V_{0P})	250 V
Maximum output voltage of DC-source (V_0)	400 V
Command output voltage	225 V
The shoot-through time duty ratio (M_{sr})	0.1

Table 2. Calculate results of MSVM and SBC.

Parameter	MSVM	SBC
$(THD)_I$	0.85	1.1
$(THD)_D$	5.95	12.11
$\hat{v}_i\,(V)$	500	500
$V_c\,(V)$	450	450
$I_L\,(A)$	10.8	10.8
$(TSDP)_{av}\,(VA)$	8876.3116	9237.6003
$(TSDP)_{pk}\,(VA)$	33322.2025	33952.7717
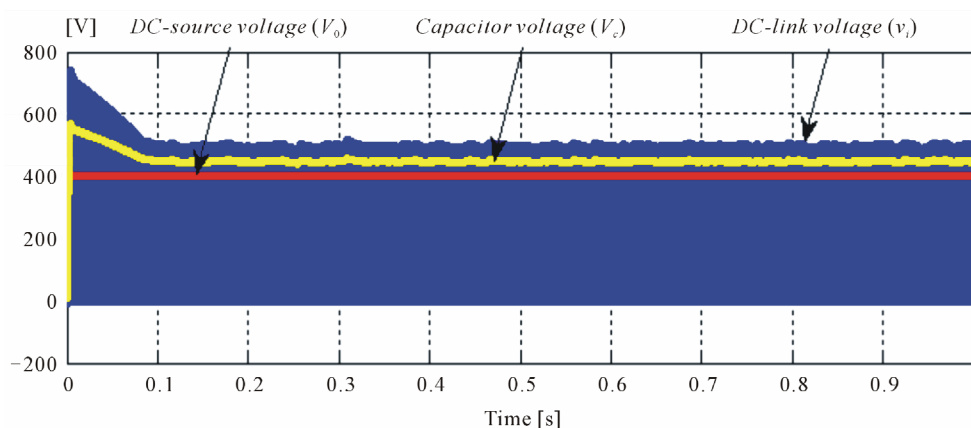
Figure 6. Simulation MSVM. DC-link voltage (v_i), Capacitor voltage (V_c) and DC-source voltage (V_0).

EPE
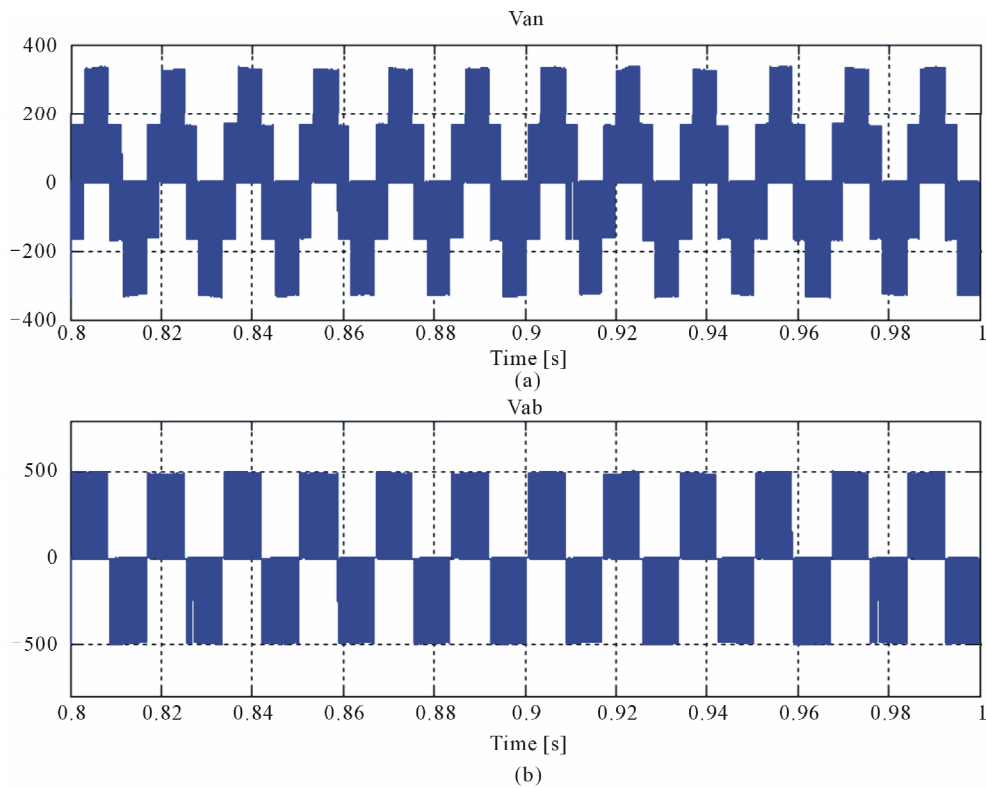
Figure 7. Switching output line voltage and phases voltage waveform of ZSI (MSVM). (a) Switching output phase voltage; (b) Switching output line voltage.
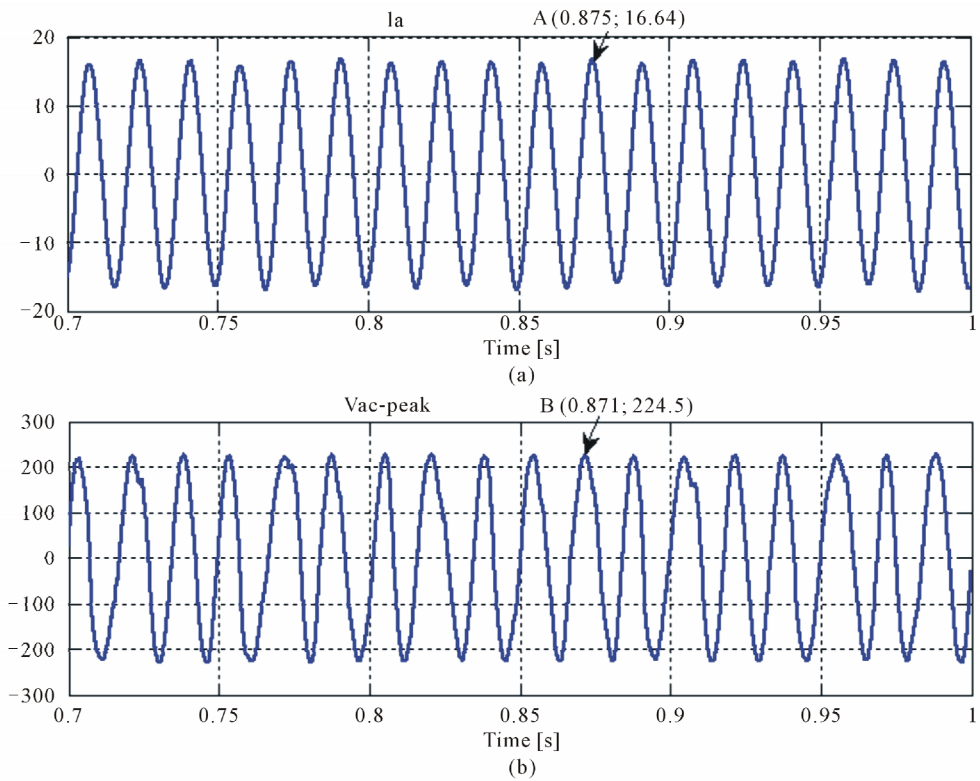
Figure 8. Output line voltage and current sine wave-forms of ZSI (MSVM). (a) Output current sine wave-forms; (b) Output line voltage sine waveforms.
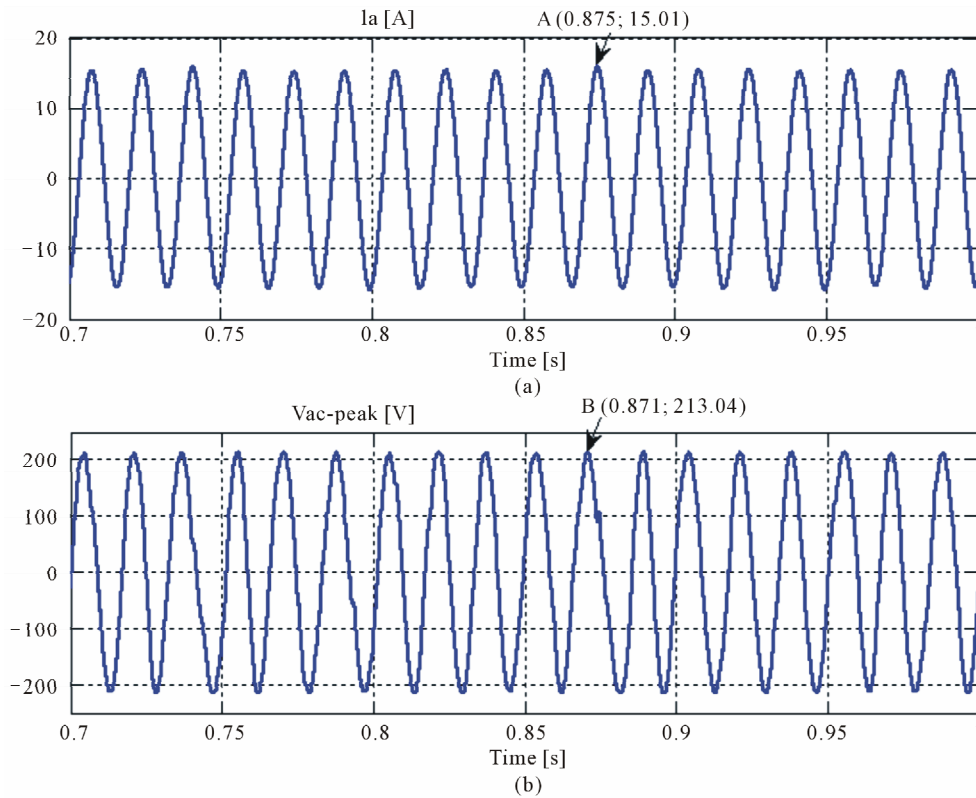
Figure 9. Output line voltage and current wave-forms of ZSI (SBC). (a) Output current; (b) Output line voltage.
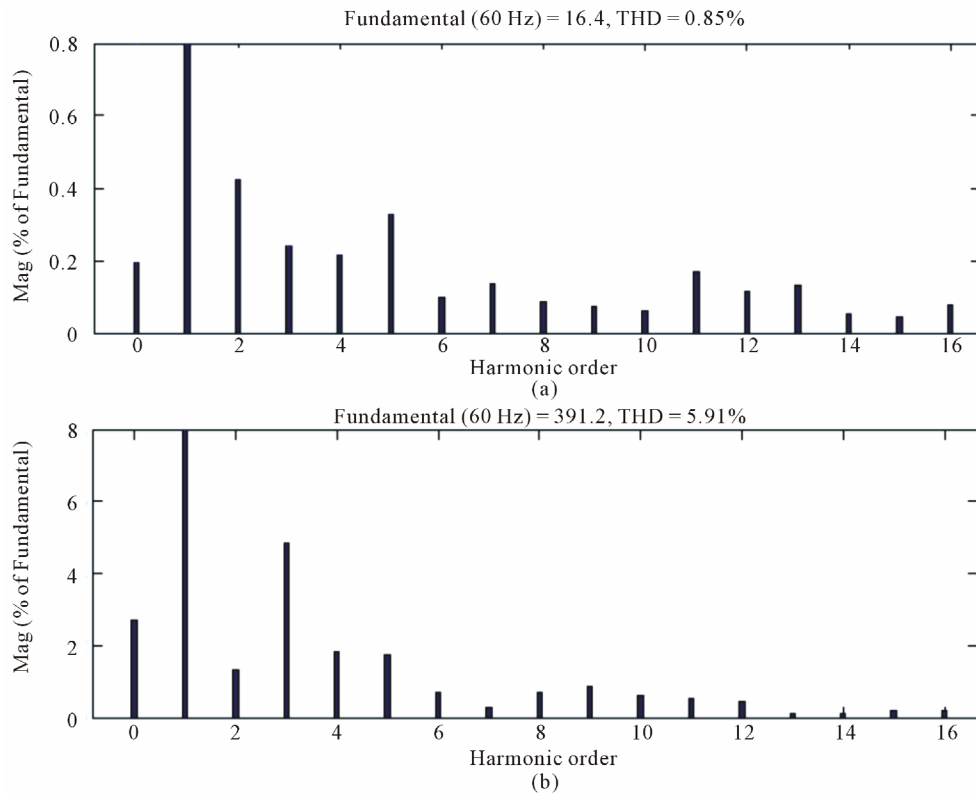
Figure 10. Harmonic spectra of Z-source inverter (MSVM). (a) Harmonic spectra of output current; (b) Harmonic spectra of output line voltage.
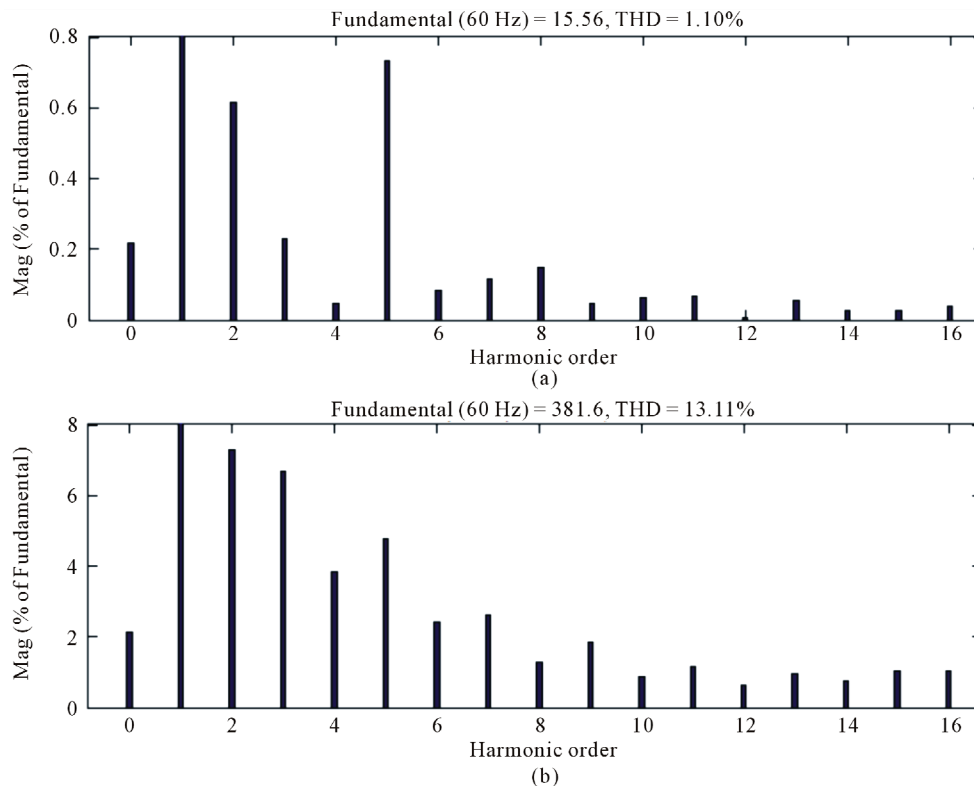
Figure 11. Harmonic spectra of Z-source inverter (SBC). (a) Harmonic spectra of output current; (b) Harmonic spectra of output line voltage.

Figure 12. The figure experiments for motor speed control system.

logy (HUST), Wuhan 430074, China. Especially, professor Anwen Shen, associate professor Phan Quoc Dzung, and master Nguyen Bao Anh who offers me advice and help me to finish this paper.

6. Conclusion

This paper presents a comparison of two different MM there are MSVM and the SBC for ZSI. They show the

harmonic spectra of output voltage and output current with MSVM is less than harmonic spectra of output voltage and output current with SBC, the total average and peak switching device power of ZSI system with MSVM method is less than the total average and peak switching device power of ZSI system with SBC, the MSVM modulation index in linear can exceed more than the SBC. All of these comparisons are used simulation MATLAB/Simulink.

REFERENCES

[1]   I. P. C. Loh, D. M. Vilathgamuwa, I. Senior, Y. S. Lai, G. T. Chua and I. Y. W. Li, "Pulse-Width Modulation of Z-Source Inverters," *IEEE Transactions on Power Electronics*, Vol. 20, No. 6, 2005, pp. 1346-1355. doi:10.1109/TPEL.2005.857543

[2]   M. Olzwesky, "Z-Source Inverter for Fuel Cell Vehicles," US Department of Energy, Freedom CAR and Vehicles Technologies, EE-2G, Washington, 2005.

[3]   K. Holland, M. Shen and F. Z. Peng, "Z-Source Inverter Control for Traction Drive of Fuel Cell-Battery Hybrid Vehicles," *Industry Applications Conference*, 40*th IAS Annual Meeting*, Vol. 3, No. 4, 2005, pp. 1651-1656.

[4]   I. Fang and Z. Peng, "Z-Source Inverter," *IEEE Transactions Industry Applications*, Vol. 39, No. 2, 2003, pp. 990-997.

[5]   J. Li, K. Q. Qu, X. L. Song and G. C. Chen, "Study on

Control Methods of Direct-Drive Wind Generation System Based on Three-Phase Z-Source Inverter," *IPEMC*, Shanghai, 17-20 May 2009.

[6] S. A. K. H. Mozafari Niapoor, S. Danyali and M. Sharifian, "Photovoltaic Power System Based mppt Z-Source Inverter to Supply a Sensorless BLDC Motor," 1*st Power Electronic*, *Drive Systems and Technologies Conference*, University of Tabriz, Tabriz, 17-18 February 2010.

[7] U. Ali and V. Kamaraj, "A Novel Space Vector pwm for Z-Source Inverter," *Proceedings of ICETECT*, Nagercoil, 23-24 March 2011.

[8] M. Shen, A. Joseph, J. Wang, F. Z. Peng and D. J. Adams, "Comparison of Traditional Inverters and Z-Source Inverter for Fuel Cell Vehicles," *IEEE Power Electronics Society*, Vol. 22, No. 4, 2007, pp. 1453-1500. doi:10.1109/TPEL.2007.900505

[9] T. Chun, Q. Tran, J. Ahn and J. Lai, "Ac Output Voltage Control with Minimization of Voltage Stress across Devices in the Z-Source Inverter Using Modified svpwm," *PESC* 37*th IEEE*, Jeju, 18-22 June 2006, pp. 1-5.

[10] B. K. Bose, "Modern Power Electronics and AC Drivers," Pearson Education, Upper Saddle River, 2002.